arXiv:1704.06272v1 [cond-mat.stat-mech] 20 Apr 2017

Generic dynamical features of quenched interacting quantum systems: survival probability, density imbalance and out-of-time-ordered correlator

E. J. Torres-Herrera,[1] Antonio M. García-García,[2] and Lea F. Santos[3]

[1]*Instituto de Física, Benemérita Universidad Autónoma de Puebla, Apt. Postal J-48, Puebla, Puebla, 72570, Mexico*
[2]*TCM Group, Cavendish Laboratory, University of Cambridge, JJ Thomson Avenue, Cambridge, CB3 0HE, UK*
[3]*Department of Physics, Yeshiva University, New York, New York 10016, USA*

We study numerically and analytically the quench dynamics of isolated many-body quantum systems out of equilibrium. Using full random matrices from the Gaussian orthogonal ensemble, we obtain analytical expressions for the evolution of the survival probability, density imbalance, and out-of-time-ordered correlator. They are compared with numerical results for a one-dimensional disordered model with two-body interactions and shown to bound the decay rate of this realistic system. Power-law decays are seen at intermediate times and overshoots beyond infinite time averages occur at long times when the system exhibits level repulsion. The fact that these features are shared by both the random matrix and the realistic disordered model indicates that they are generic to nonintegrable interacting quantum systems out of equilibrium.

Nonequilibrium dynamics of isolated many-body quantum systems is a highly interdisciplinary subject covering a broad range of physics scales, from string theory and black holes to condensed matter and atomic physics. The connection between black hole physics and unitary quantum dynamics emerges from holographic dualities [1]. On the experimental side, unitary quantum dynamics is investigated with cold atoms [2–5], ion traps [6, 7], and nuclear magnetic resonance platforms [8, 9].

Motivated by different goals, studies of black hole information loss [10–12], quantum chaos [13, 14], thermalization in isolated quantum systems [2, 5, 15], many-body localization [3, 9, 16], quantum correlations [8], and quantum speed limits [17–19] consider similar dynamical quantities. They include the survival probability, density imbalance, and out-of-time-ordered correlator (OTOC). Our goal is to characterize the evolution of these quantities at different time scales.

Given the complexity of out-of-equilibrium many-body quantum systems, we take the same approach as Wigner when studying heavy nuclei and use full random matrices (FRM) from the Gaussian orthogonal ensemble (GOE). These are matrices filled with random real numbers and constrained by time-reversal symmetry. The model is unrealistic, as it assumes simultaneous and infinite-range interactions among all particles. But it allows for the derivation of analytical expressions for the observables of interest.

We compare the analytical expressions with numerical results for the one-dimensional (1D) Heisenberg spin-1/2 model with onsite disorder. This system has been extensively studied in the context of many-body localization [20–22]. It shows a chaotic regime for small disorder [23, 24], which justifies the comparison with FRM. The rate of the evolution is faster in the FRM case, but the overall dynamical behavior is very similar for both models. This suggests that analytical results obtained with FRM can assist in the identification of general features and bounds for the dynamics of realistic interacting systems out of equilibrium.

The basis of our analysis is the survival probability. It gives the probability of finding the initial state later in time and has been investigated since the early days of quantum mechanics [25]. It is a main quantity in the studies of quantum speed limits [19] and decay processes of unstable systems [26]. More recently, it became central to the analysis of localization in noninteracting [27, 28] and interacting [29, 30] systems. The survival probability is also related [31] to the analytic continuation of the partition function used to study conformal field theories with holographic duals [32] and to describe the time behavior of large anti-de Sitter black holes [11, 12, 33].

Our analytical expression for the survival probability for the FRM model covers the entire duration of the evolution. Following the same steps for its derivation, we find analytical expressions for the density imbalance and OTOC. The density imbalance is measured in experiments with cold atoms [3, 4]. The OTOC [14] quantifies the degree of non-commutativity in time between two Hermitian operators that commute at time $t = 0$ and has been studied experimentally [8]. The results for the survival probability can be employed also to describe the growth of the information and entanglement entropies [34].

The short-time dynamics of the survival probability is controlled by the Fourier transform of the envelope of the energy distribution of the initial state, the so-called local density of states (LDOS). When the perturbation that takes the system out of equilibrium is strong, the LDOS is similar to the density of states (DOS). The DOS for the FRM has a semicircle shape, which leads to a decay $\propto \mathcal{J}_1(t)^2/t^2$, where $\mathcal{J}_1(t)$ is the Bessel function of first kind [35–37]. The initial decay of the density imbalance follows the same behavior, while the OTOC goes as $\mathcal{J}_1(t)^4/t^4$. For the spin system, where only two-body interactions exist, the decay is slower. In this case, maximally spread-out LDOS reach Gaussian shapes, resulting in Gaussian decays [35–39].

The envelope of the oscillations of the term involving the Bessel function decays as $1/t^3$ for the survival probability [40–42] and imbalance, and as $1/t^6$ for the OTOC. These behaviors emerge when the tails of the DOS fall with the square root of the energy [41, 42]. The same power-law exponents are found in the Sachdev-Ye-Kitaev (SYK) model [12, 43], where the DOS is also semicircle at the edges [44, 45]. In the spin model, the tails of the LDOS decay slowly to its energy bounds, which yields smaller power-law exponents.

For long times, but still shorter than the inverse of the mean

level spacing (Heisenberg time), the survival probability for both the FRM and the spin model shows a dip below its saturation value, known as correlation hole [46–49]. This is an explicit dynamical manifestation of level repulsion in systems with discrete spectra [30, 50]. For yet longer times, the survival probability eventually saturates. Its increase from the bottom of the hole to saturation is nearly linear and very similar for both models. The correlation hole appears also for the imbalance and OTOC, and it causes overshoots in the increase of the information and entanglement entropies [50].

Hamiltonians and Dynamical Quantities.– We consider Hamiltonians H that have an unperturbed part H_0 and a perturbation V of strength J, that is $H = H_0 + JV$. The energy scale is set by choosing $J = 1$.

For the 1D spin-1/2 model with onsite disorder, L sites, and periodic boundary conditions, $H_0 = \sum_{k=1}^{L} h_k S_k^z$ and $V = \sum_{k=1}^{L} \vec{S}_k \vec{S}_{k+1}$, where $\vec{S}_k$ are the spin operators on site k and $\hbar = 1$. The amplitudes h_k of the random static magnetic fields are random numbers from a uniform distribution $[-h, h]$. The total spin in the z-direction, $\mathcal{S}^z = \sum_k S_k^z$, is conserved. We study the largest subspace, $\mathcal{S}^z = 0$, which has dimension $\mathcal{N} = L!/(L/2)!^2$.

When $h = 0$ or $h > h_c$, where h_c is the critical point above which the system becomes spatially localized, the eigenvalues can cross and the distribution of the spacings of neighboring levels is Poisson, as typical of integrable models. For $0 < h < h_c$, the eigenvalues become correlated and repel each other. The level spacing distribution is intermediate between Wigner-Dyson and Poisson. The best agreement with Wigner-Dyson distribution for $\mathcal{N} = 12870$ occurs at $h \sim 0.5$ [30].

In the FRM model, H_0 is the diagonal part of the matrix and V consists of the off-diagonal elements. In FRM from the GOE, the matrix elements H_{nm} are random numbers from a Gaussian distribution with mean zero. The variance of the elements of V is σ^2 and for H_0, $2\sigma^2$. The rotational symmetry imposes that $H_{nm} = H_{mn} = H_{mn}^*$ [51]. As in the spin model, $\mathcal{N}$ is the size of the matrix.

The system is initially in an eigenstate $|\phi_n\rangle$ of H_0. The dynamics starts by switching on the perturbation abruptly. The evolution of the initial state $|\Psi(0)\rangle$ is then dictated by H, $|\Psi(t)\rangle = e^{-iHt}|\Psi(0)\rangle$. The eigenstates and eigenvalues of H are denoted by $|\psi_\alpha\rangle$ and E_α. The dynamical quantities investigated are listed below.

(i) The survival probability is given by

$$W_{n_0}(t) = |\langle\Psi(t)|\Psi(0)\rangle|^2 = \left|\sum_\alpha \left|C_{n_0}^{(\alpha)}\right|^2 e^{-iE_\alpha t}\right|^2, \quad (1)$$

where $C_{n_0}^{(\alpha)} = \langle\psi_\alpha|\Psi(0)\rangle$.

(ii) The imbalance of the spin density for all sites is computed as in [52, 53],

$$I(t) = \frac{4}{L}\sum_{k=1}^{L}\langle\Psi(0)|S_k^z(0)S_k^z(t)|\Psi(0)\rangle. \quad (2)$$

(iii) The OTOC corresponds to

$$O_{toc}(t) = \langle O_1^\dagger(t)O_2^\dagger(0)O_1(t)O_2(0)\rangle_\beta, \quad (3)$$

where $O_1(t) = e^{iHt}O_1(0)e^{-iHt}$ and $\langle.\rangle_\beta$ denotes the average over a thermal ensemble at temperature $1/\beta$. We choose $O_1 = S_{k'}^z$ and $O_2 = S_k^z$. All states of the subspace $\mathcal{N}$ are assumed to contribute equally, similarly to what was done in [16].

Survival Probability.– We can write Eq. (1) in terms of the Fourier transform of the spectral autocorrelation function as $W_{n_0}(t) = \int G(E)e^{-iEt}dE + \overline{W}_{n_0}$, where $\overline{W}_{n_0} = \sum_\alpha |C_{n_0}^{(\alpha)}|^4$ is the infinite time average and $G(E) = \sum_{\alpha_1\neq\alpha_2} |C_{n_0}^{(\alpha_1)}|^2|C_{n_0}^{(\alpha_2)}|^2\delta(E - E_{\alpha_1} + E_{\alpha_2})$.

In the GOE FRM model, the eigenstates are random vectors, so $\langle\overline{W}_{n_0}\rangle_{\text{FRM}} = 3/(\mathcal{N}+2)$, where $\langle.\rangle_{\text{FRM}}$ represents the ensemble average. Since the eigenvalues and eigenstates are statistically independent, $G(E)$ can be separated into $\langle\sum_{\alpha_1\neq\alpha_2}|C_{n_0}^{(\alpha_1)}|^2|C_{n_0}^{(\alpha_2)}|^2\rangle_{\text{FRM}} = 1 - \overline{W}_{n_0}$ and $\langle\delta(E - E_{\alpha_1} + E_{\alpha_2})\rangle_{\text{FRM}} = \int\delta(E - E_{\alpha_1} + E_{\alpha_2})R_2(E_{\alpha_1}, E_{\alpha_2})dE_{\alpha_1}dE_{\alpha_2}/[\mathcal{N}(\mathcal{N}-1)]$, where $R_2(E_{\alpha_1}, E_{\alpha_2})$ is the 2-point correlation function. R_2 splits in the 1-point correlation function, which is simply the DOS, and the 2-level cluster function [54]. As $\mathcal{N}\to\infty$, the DOS converges to the Wigner semicircle law, $\rho(E) = \frac{2\mathcal{N}}{\pi\varepsilon}\sqrt{1-\left(\frac{E}{\varepsilon}\right)^2}$, where 2ε is the length of the spectrum.

The Fourier transform of the semicircle leads to a term $\propto \mathcal{J}_1(\varepsilon t)/t$ [35]. The Fourier transform of the 2-level cluster function gives the 2-level form factor $b_2(Dt/2\pi)$, where D is the mean level spacing [51, 54]. In the large $\mathcal{N}$ limit, $D \approx 1/\rho(0)$. Therefore,

$$W_{n_0}^{\text{FRM}}(t) = \frac{1-\overline{W}_{n_0}}{\mathcal{N}-1}\left[4\mathcal{N}\frac{\mathcal{J}_1^2(\varepsilon t)}{(\varepsilon t)^2} - b_2\left(\frac{\varepsilon t}{4\mathcal{N}}\right)\right] + \overline{W}_{n_0}, \quad (4)$$

where $b_2(\overline{t}) = [1-2\overline{t}+\overline{t}\ln(1+2\overline{t})]\Theta(1-\overline{t}) + \{-1+\overline{t}\ln[(2\overline{t}+1)/(2\overline{t}-1)]\}\Theta(\overline{t}-1)$ and Θ is the Heaviside step function.

In Fig. 1 (a), we compare Eq. (4) with the numerical results for the GOE FRM. The agreement is excellent, the two curves can hardly be distinguished. The initial dynamics is controlled by the term with the Bessel function, which leads to oscillations that decay as $1/t^3$ (dashed line) [41, 42].

The correlation hole develops after the power-law decay and is caused by $b_2(\overline{t})$. The time evolution in this region is a direct probe of long-range eigenvalue correlations. For level statistics given by the Poisson distribution, the correlation hole is nonexistent, since $b_2(\overline{t}) = 0$. As we approach the Heisenberg time, the hole fades aways and the dynamics eventually saturates at $\overline{W}_{n_0}$ (dot-dashed line).

In Fig. 1 (b), we compare Eq. (4) (dotted line) with numerical results for the analytic continuation of the partition function, $|Z(\beta+it)|^2 = \sum_\alpha \exp[-(\beta+it)E_\alpha]/Z(\beta)$ (solid lines). As discussed in Ref. [31], $|Z(\beta+it)|^2$ is analogous to the survival probability if one considers as initial state, a thermofield state, that is $|\Psi(0)\rangle = \sum_\alpha \exp(-\beta E_\alpha/2)|\psi_\alpha\rangle/\sqrt{Z(\beta)}$. As illustrated in Fig. 1 (b), the results for $|Z(\beta+it)|^2$ using the eigenvalues E_α from GOE FRM and the coefficients $C_{n_0}^{(\alpha)}$ from the thermofield state show qualitative agreement with $W_{n_0}^{\text{FRM}}(t)$. The survival probability and $|Z(\beta+it)|^2$ for $\beta = 0$ decay initially as $\mathcal{J}_1^2(\varepsilon t)/(\varepsilon t)^2$ and all curves show a correlation hole. However, this comparison has limitations, since

$C_{n_0}^{(\alpha)}$ in the context of quench dynamics cannot be chosen independently of H_0 and H. Contrary to $|Z(\beta+it)|^2$, $W_{n_0}(t)$ depends on the quench protocol.

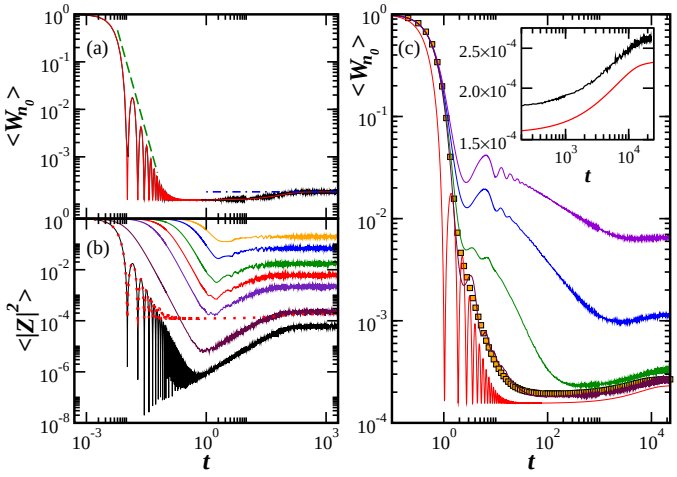

FIG. 1: Survival probability and $|Z(\beta+it)|^2$. In (a): GOE FRM. Numerical results and Eq. (4) are superposed; $1/t^3$ decay (dashed), saturation value (dot-dashed). In (b), solid lines from bottom to top give $|Z(\beta+it)|^2$ with $\beta = 0, 0.01, 0.05, 0.1, 0.2, 0.5, 1$; dotted curve is Eq. (4). In (c), solid lines from bottom to top are: Eq. (4) and numerical results for the disordered model with $h = 0.5, 1, 1.5, 2$. Squares correspond to the fitting curve for $h = 0.5$. The FRM is rescaled, so the DOS of both models have the same width. Inset of (c): growth of $W_{n_0}(t)$ to saturation; Eq. (4) (bottom) and time average for $h = 0.5$ (top). In (a,b): averages over 200 disorder realizations, $\mathcal{N} = 16\,384$, $\sigma^2 = 2$. In (c): average over 10^5 data, $\mathcal{N} = 12\,870$.

Figure 1 (c) depicts the survival probability for the spin model with different disorder strengths. The result is averaged over disorder realizations and $0.1\mathcal{N}$ initial states with energy in the middle of the spectrum. Even deep in the chaotic regime ($h = 0.5$), the decay is slower than that for the FRM model, being bounded by Eq. (4). This is caused by two related factors: the Gaussian shape of the DOS [55] and the lack of full ergodicity of the eigenstates of the realistic system, which approach random vectors only away from the spectrum borders.

To make the comparison between the two models more explicit, we fit the curve for $h = 0.5$ taking into account the following features of the realistic system: (i) the Fourier transform of a Gaussian LDOS leads to a Gaussian decay at short times, $e^{-w^2t^2}$, where w is the width of the LDOS [35–39], (ii) due to the energy bounds of the spectrum, the behavior later becomes power-law and $\propto 1/t^2$ [41, 42]; (iii) the presence of level repulsion induces the correlation hole at long times. These three items, together with the eventual saturation of $W_{n_0}(t)$, motivate the expression $W_{n_0}(t) = \frac{1-\overline{W}_{n_0}}{\mathcal{N}-1}\left[\mathcal{N}\frac{g(t)}{g(0)} - b_2\left(\frac{wt}{\mathcal{N}}\right)\right] + \overline{W}_{n_0}$, where $g(t) = e^{-w^2t^2} + A(1-e^{-w^2t^2})/(w^2t^2)$ and A is the only fitting constant. As seen in Fig. 1 (c), this expression captures very well the behavior of $W_{n_0}(t)$ for $h = 0.5$.

The inset of Fig. 1 (c) confirms that b_2 is the appropriate function to describe the correlation hole also for the realistic chaotic system. The inset shows the growth of $W_{n_0}(t)$ from the deepest value of the hole to saturation. The $h = 0.5$ curve follows closely the FRM analytical expression of b_2.

Despite unrealistic, the FRM model provides useful insights into the dynamical behavior of realistic many-body quantum systems. With it, one can extract the main features of generic interacting systems and use them to propose fitting curves, as successfully done in Fig. 1 (c).

The $1/t^3$ decay obtained with the FRM model is observed also for the SYK model [12] and for $1+1$ dimensional conformal field theories with a gravity-dual [32]. Since field theories with holographic dual set bounds to certain dynamical coefficients [56], one may speculate whether the $1/t^3$ behavior is a general bound to the decay of the survival probability and related quantities of generic lattice many-body quantum systems. The origin of the $1/t^3$ decay is the square-root edge of the DOS. But if we replace the Gaussian distribution of the random entries of the FRM by distributions involving higher even powers, it is possible to achieve DOS whose tails go as $|E-E_0|^\xi$ where $\xi = 3/2, 5/2, \ldots$ and E_0 is the edge of the spectrum [57], which would lead to decays faster than $1/t^3$. Whether there may be realistic systems with such DOS is an open question. Decays faster than $1/t^3$ have been observed in realistic systems that are either integrable [58] or have few particles [59], none of these cases are related to the nonintegrable many-body quantum systems treated here.

Density Imbalance.– Level repulsion manifests itself not only as the correlation hole of the survival probability. It is revealed also in the long-time evolution of observables such as the spin density imbalance.

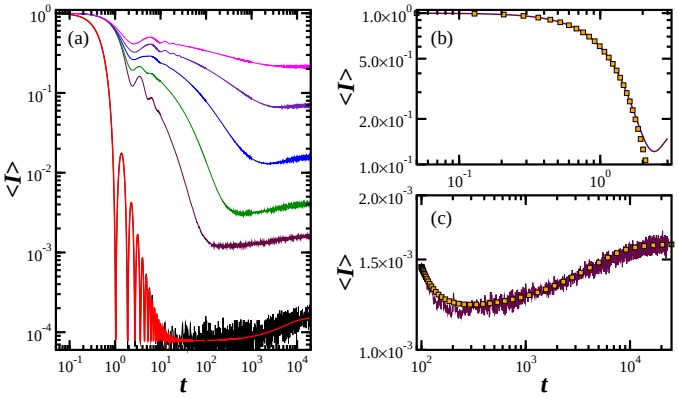

FIG. 2: Density imbalance for FRM and disordered spin model. In (a) from bottom to top: FRM (numerical and analytical curves) and disorder strength $h = 0.5, 1, 1.5, 2, 2.5$. In (b) and (c): numerical result (solid) and fitting (squares) for $h = 0.5$. In (b): short-time dynamics with Gaussian behavior. In (c): long-time evolution fitted with a power-law decay and the $b_2(\overline{t})$ function. Averages over 10^4 random realizations, $\mathcal{N} = 12\,870$.

The curves for the density imbalance for the FRM model and for the disordered spin system with different values of h show a dip below the saturation value, as illustrated in Fig. 2 (a). As h increases above 0.5 and the system moves away from the chaotic region, the dip gets less deep, the time interval of its existence shrinks, and the moment when it first appears gets deferred to longer times. This is consistent with the fact that

the long-range eigenvalue correlations diminish as the realistic system moves away from the chaotic region.

The analytical expression for a general observable O can be derived from $O(t) = \int K(E)e^{-iEt}dE + \overline{O}$, where $K(E) = \sum_{\alpha_1\neq\alpha_2} C_{n_0}^{(\alpha_1)}C_{n_0}^{(\alpha_2)}O_{\alpha_1\alpha_2}\delta(E-E_{\alpha_1}+E_{\alpha_2})$ with $O_{\alpha_1\alpha_2} = \langle\psi_{\alpha_1}|O|\psi_{\alpha_2}\rangle$, and $\overline{O} = \sum_\alpha |C_{n_0}^{(\alpha)}|^2 O_{\alpha\alpha}$ is the infinite time average.

In the FRM model, where the eigenvalues, eigenstates, and $O_{\alpha_1\alpha_2}$ are statistically independent, we can separate $K(E)$ into $\langle\sum_{\alpha_1\neq\alpha_2} C_{n_0}^{(\alpha_1)}C_{n_0}^{(\alpha_2)}O_{\alpha_1\alpha_2}\rangle_{\rm FRM} = O(0)-\overline{O}$ and $\langle\delta(E-E_{\alpha_1}+E_{\alpha_2})\rangle_{\rm FRM}$, which was already computed for Eq. (4). This leads to the following expression for the density imbalance,

$$I^{\rm FRM}(t) = \frac{I(0)-\overline{I}}{\mathcal{N}-1}\left[4\mathcal{N}\frac{\mathcal{J}_1^2(\varepsilon t)}{(\varepsilon t)^2} - b_2\left(\frac{\varepsilon t}{4\mathcal{N}}\right)\right] + \overline{I}, \quad (5)$$

where $\overline{I} = 2I(0)/(\mathcal{N}+2)$. The result is very similar to that for the survival probability, leading also to the $1/t^3$ decay of the oscillations, as seen in Fig. 2 (a).

The decay of the imbalance for the disordered model is bounded by Eq. (5) and it follows a power-law behavior even deep in the chaotic domain. Algebraic decays have been much explored in studies of many-body localization, but they are not exclusive to systems in the vicinity of a localized phase.

The relaxation of $I(t)$ for the disordered spin model was investigated in [52]. There, a fitting function with 9 free parameters was proposed for the intermediate times, where the power-law behavior is observed. We add to this picture the description of the short- and long-time dynamics.

The imbalance for the spin system follows closely what happens for the survival probability. The initial decay, up to $wt \sim 2$, is Gaussian. This is shown in Fig. 3 (b) with the numerical result and a Gaussian fitting function.

The correlation hole emerges at long times and is shown in Fig. 3 (c). The numerical curve for $h = 0.5$ is fitted with the function $At^{-B} - Cb_2\left(\frac{wt}{\mathcal{N}}\right)$, where A, B, and C are fitting constants. We use the same $b_2(\overline{t})$ from the fitting for the survival probability in Fig. 2 (c). The agreement is very good, covering a large time interval all the way to saturation.

Out-of-time-ordered correlator.– Analogously to what happens for the density imbalance, the evolution of the OTOC for the FRM model is initially very fast, but later slows down and decays as $1/t^6$. The OTOC involves the 4-point correlation function $R_4(E_{\alpha_1}, E_{\alpha_2}, E_{\alpha_3}, E_{\alpha_4})$ derived from the ensemble average $\langle\delta(E-E_{\alpha_1}+E_{\alpha_2}-E_{\alpha_3}+E_{\alpha_4})\rangle_{\rm FRM}$. R_4 can be expressed as the determinant of a single spectral kernel which is known explicitly [54]. For short and intermediate times, the leading contribution to the Fourier transform of R_4 is proportional to $\mathcal{J}_1^4(\varepsilon t)/(\varepsilon t)^4$, which causes the $1/t^6$ decay. At long times, $b_2^2(Dt/2\pi)$ becomes dominant and causes the correlation hole.

In Fig. 3 (a), we show the $1/t^6$ behavior of the OTOC. The agreement between the numerical data and the analytical prediction from FRM is very good. In Fig. 3 (b), the analytical curve for the FRM model is compared with the decay for the disordered spin system with $h = 0.5$. The decay of the latter is slower and exhibits a Gaussian behavior for short times.

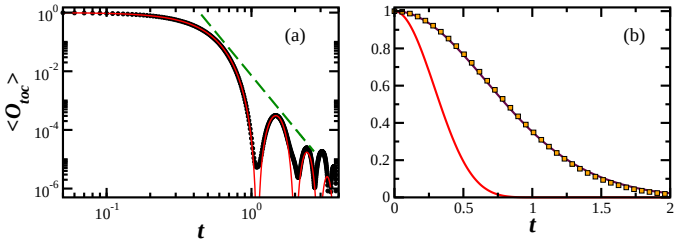

FIG. 3: OTOC for FRM (a) and compared with the disordered model for $h = 0.5$ (b). In (a): $\mathcal{J}_1^4(\varepsilon t)/(\varepsilon t)^4$ (solid), numerical results (circles), $1/t^6$ (dashed). In (b): FRM (bottom) and $h = 0.5$ (top); numerical curve (solid) and Gaussian fit (squares). Averages over 340 (FRM) and 100 (spin model) disorder realizations; $\mathcal{N} = 3432$.

The survival probability, and therefore also $I(t)$ and $O_{toc}(t)$, are not self-averaging [60]. The number of random matrices used in the ensemble average for the imbalance to reasonably expose the correlation hole was much larger than what was needed to get a smooth curve for the survival probability. Even larger ensembles should be needed for the OTOC.

Conclusion.– We have found analytical expressions for the evolution of the survival probability, density imbalance, and OTOC for a FRM model. These observables are central to studies of quantum systems out of equilibrium. The analytical findings were compared with numerical results for a 1D disordered spin-1/2 system away from localization. The power-law decays, for intermediate times, and dips below the saturation values, for longer times, revealed by the FRM model appeared also for the spin model. The identification of these generic properties help us finding and justifying the functions that best match the dynamics of the disordered model and, by extension, of equivalent lattice many-body quantum systems with two-body interactions and level repulsion.

Acknowledgments.– EJTH acknowledges funding from CONACyT and VIEP-BUAP, Mexico. He is also grateful to LNS-BUAP for allowing use of their supercomputing facility. AMG acknowledges partial financial support from a QuantEmX grant from ICAM and the Gordon and Betty Moore Foundation through Grant GBMF5305. LFS was supported by the NSF grant No. DMR-1603418.

[1] J. Maldacena, Adv. Theor. Math. Phys. **2**, 231 (1998).
[2] T. Kinoshita, T. Wenger, and D. S. Weiss, Nature **440**, 900 (2006).
[3] M. Schreiber, S. S. Hodgman, P. Bordia, H. P. Lüschen, M. H. Fischer, R. Vosk, E. Altman, U. Schneider, and I. Bloch, Science **349**, 842 (2015).
[4] P. Bordia, H. Lüschen, S. Scherg, S. Gopalakrishnan, M. Knap, U. Schneider, and I. Bloch, arXiv:1704.03063.

[5] A. M. Kaufman, A. L. M. Eric Tai, M. Rispoli, R. Schittko, P. M. Preiss, and M. Greiner, Science **353**, 794 (2016).

[6] P. Jurcevic, B. P. Lanyon, P. Hauke, C. Hempel, P. Zoller, R. Blatt, and C. F. Roos, Nature **511**, 202 (2014).

[7] J. Smith, A. Lee, P. Richerme, B. Neyenhuis, P. W. Hess, P. Hauke, M. Heyl, D. A. Huse, and C. Monroe, Nat. Phys. **12**, 907 (2016).

[8] M. Gärttner, J. G. Bohnet, A. Safavi-Naini, M. L. Wall, J. J. Bollinger, and A. M. Rey, arXiv:1608.08938.

[9] K. X. Wei, C. Ramanathan, and P. Cappellaro, arXiv:1612.05249.

[10] D. A. Roberts, D. Stanford, and L. Susskind, JHEP **2015**, 51 (2015), ISSN 1029-8479.

[11] K. Papadodimas and S. Raju, Phys. Rev. Lett. **115**, 211601 (2015).

[12] J. S. Cotler, G. Gur-Ari, M. Hanada, J. Polchinski, P. Saad, S. H. Shenker, D. Stanford, A. Streicher, and M. Tezuka, arXiv:1611.04650.

[13] D. A. Roberts and D. Stanford, Phys. Rev. Lett. **115**, 131603 (2015).

[14] J. Maldacena, S. H. Shenker, and D. Stanford, JHEP **2016**, 106 (2016).

[15] F. Borgonovi, F. M. Izrailev, L. F. Santos, and V. G. Zelevinsky, Phys. Rep. **626**, 1 (2016).

[16] R. Fan, P. Zhang, H. Shen, and H. Zhai, arXiv:1608.01914.

[17] L. Mandelstam and I. Tamm, J. Phys. USSR **9**, 249 (1945).

[18] N. Margolus and L. B. Levitin, Physica D **120**, 188 (1998).

[19] J. G. Muga, A. Ruschhaupt, and A. del Campo, *Time in Quantum Mechanics, vol. 2* (Springer, London, 2009).

[20] L. F. Santos, G. Rigolin, and C. O. Escobar, Phys. Rev. A **69**, 042304 (2004).

[21] F. Dukesz, M. Zilbergerts, and L. F. Santos, New J. Phys. **11**, 043026 (2009).

[22] R. Nandkishore and D. Huse, Annu. Rev. Condens. Matter Phys. **6**, 15 (2015).

[23] Y. Avishai, J. Richert, and R. Berkovitz, Phys. Rev. B **66**, 052416 (2002).

[24] L. F. Santos, J. Phys. A **37**, 4723 (2004).

[25] L. A. Khalfin, Sov. Phys. JETP **6**, 1053 (1958).

[26] L. Fonda, G. C. Ghirardi, and A. Rimini, Rep. Prog. Phys., **41**, 587 (1978).

[27] R. Ketzmerick, G. Petschel, and T. Geisel, Phys. Rev. Lett. **69**, 695 (1992).

[28] B. Huckestein and L. Schweitzer, Phys. Rev. Lett. **72**, 713 (1994).

[29] E. J. Torres-Herrera and L. F. Santos, Phys. Rev. B **92**, 014208 (2015).

[30] E. J. Torres-Herrera and L. F. Santos, Ann. Phys. (Berlin) p. 1600284 (2017), ISSN 1521-3889.

[31] A. del Campo, J. Molina-Vilaplana, and J. Sonner, arXiv:1702.04350.

[32] E. Dyer and G. Gur-Ari, arXiv:1611.04592.

[33] J. M. Maldacena, JHEP **04**, 021 (2003), hep-th/0106112.

[34] E. J. Torres-Herrera, J. Karp, M. Távora, and L. F. Santos, Entropy. **18**, 359 (2016).

[35] E. J. Torres-Herrera and L. F. Santos, Phys. Rev. A **89**, 043620 (2014).

[36] E. J. Torres-Herrera, M. Vyas, and L. F. Santos, New J. Phys. **16**, 063010 (2014).

[37] E. J. Torres-Herrera and L. F. Santos, Phys. Rev. A **90**, 033623 (2014).

[38] E. J. Torres-Herrera and L. F. Santos, Phys. Rev. E **89**, 062110 (2014).

[39] F. M. Izrailev and A. Castañeda-Mendoza, Phys. Lett. A **350**, 355 (2006).

[40] E. J. Torres-Herrera, D. Kollmar, and L. F. Santos, Phys. Scr. T **165**, 014018 (2015).

[41] M. Távora, E. J. Torres-Herrera, and L. F. Santos, Phys. Rev. A **94**, 041603 (2016).

[42] M. Távora, E. J. Torres-Herrera, and L. F. Santos, Phys. Rev. A **95**, 013604 (2017).

[43] D. Bagrets, A. Altland, and A. Kamenev, arXiv:1702.08902.

[44] A. M. García-García and J. J. M. Verbaarschot, Phys. Rev. D **94**, 126010 (2016).

[45] A. M. García-García and J. J. Verbaarschot, arXiv preprint arXiv:1701.06593 (2017).

[46] L. Leviandier, M. Lombardi, R. Jost, and J. P. Pique, Phys. Rev. Lett. **56**, 2449 (1986).

[47] T. Guhr and H. Weidenmüller, Chem. Phys. **146**, 21 (1990).

[48] Y. Alhassid and R. D. Levine, Phys. Rev. A **46**, 4650 (1992).

[49] T. Gorin and T. H. Seligman, Phys. Rev. E **65**, 026214 (2002).

[50] E. J. Torres-Herrera and L. F. Santos, arXiv:1702.04363.

[51] T. Guhr, A. Mueller-Gröeling, and H. A. Weidenmüller, Phys. Rep. **299**, 189 (1998).

[52] D. J. Luitz, N. Laflorencie, and F. Alet, Phys. Rev. B **93**, 060201 (2016).

[53] M. Lee, T. R. Look, D. N. Sheng, and S. P. Lim, arXiv:1703.05425.

[54] M. L. Mehta, *Random Matrices* (Academic Press, Boston, 1991).

[55] T. A. Brody, J. Flores, J. B. French, P. A. Mello, A. Pandey, and S. S. M. Wong, Rev. Mod. Phys **53**, 385 (1981).

[56] P. Kovtun, D. T. Son, and A. O. Starinets, Phys. Rev. Lett. **94**, 111601 (2005).

[57] E. Brézin, C. Itzykson, G. Parisi, and J. B. Zuber, Commun. Math. Phys. **59**, 35 (1978), ISSN 1432-0916.

[58] A. del Campo, New J. Phy. **18**, 015014 (2016).

[59] T. Taniguchi and S.-i. Sawada, Phys. Rev. E **83**, 026208 (2011).

[60] R. E. Prange, Phys. Rev. Lett. **78**, 2280 (1997).